Macromolecular Chemistry and Physic
www.mcp-journal.d

Role of High-Molecular-Weight Homopolymers on Block Copolymer Self-Assembly: From Morphology Modifier to Template

Shuo Zhang, Chunhua Cai, Zhanwen Xu, Jiaping Lin,* and Xiao Jin*

For block copolymer (BCP)/homopolymer self-assembly systems, the molecular weight of homopolymers is usually lower than that of BCPs. Herein, the cooperative self-assembly of polystyrene-*b*-poly(ethylene glycol) (PS-*b*-PEG) BCPs with high-molecular-weight polystyrene (PS) homopolymers is reported. The molecular weight of PS homopolymers is 3–63 times that of the PS blocks. Typically, a spherical micelle–vesicle–large sphere morphology transition is observed by increasing the weight fraction of PS homopolymers in the polymer mixtures (f_{HP}). Dynamic process studies reveal that with adding water to the solution of polymer mixtures in organic solvent, the homopolymers first collapse into globules, and their size increases with f_{HP} and the molecular weight. Then these PS globules cooperatively self-assemble with the PS-*b*-PEG BCPs. Depending on their size, these PS globules play different roles in the self-assembly process. Small PS globules act as morphology modifiers inducing the micelle–vesicle transition, while large PS globules serve as self-assembly templates for PS-*b*-PEG resulting in large spheres.

1. Introduction

Amphiphilic block copolymers (BCPs) are capable of self-assembling into diverse nanostructures in selective solvents.[1–6] Tuning morphology of the assembled aggregates becomes one of the key topics for BCPs self-assembly research, since the morphology of the self-assembled aggregates influences their properties and application performance.[7–11] A variety of strategies such as introducing a second component, controlling copolymer composition, and altering self-assembly condition have been applied to tune the morphology of BCP aggregates.[12–18] Hydrophobic homopolymers (HPs) have been found to be efficient morphology modifiers for BCP aggregates.[19–27] In most of the reported BCP/HP self-assembly systems, the molecular weight of the hydrophobic core-forming HPs is lower than or close to that of the core-forming blocks in BCPs. However, little is known about the cases in which the molecular weight of the core-forming HPs is much higher than that of the BCPs.

Recently, some studies indicated that when the molecular weight of homopolymers is much larger than that of the BCPs, the BCP/HP mixtures can also self-assemble into stable aggregates with novel morphologies. For example, Novak et al. reported that superhelices can be prepared from the mixtures of polycarbodiimide-*b*-poly(ethylene glycol) rod–coil BCPs and high-molecular-weight polycarbodiimide rigid HPs.[28,29] In our previous work, it was found that the mixtures of rod–coil BCPs/high-molecular-weight rigid HPs could self-assemble into helical and abacus-like fibers, and the mixtures of rod–coil BCPs/high-molecular-weight flexible HPs formed striped spheres.[30–32] It should be noted that such BCPs and high-molecular-weight HPs mixtures share a common feature, that is, the core-forming blocks and/or HPs are rigid segments. In these self-assembled aggregates, the HPs formed cylindrical or spherical cores and the BCPs formed nanostructured shells. Considering that flexible polymers are more common than rigid ones, studies on flexible polymer systems should be of more general significance. However, up to now, there is no systematic study regarding self-assembly behavior of coil–coil BCPs with high-molecular-weight core-forming flexible HPs.

Herein, we report the cooperatively self-assembly behavior of polystyrene-*b*-poly(ethylene glycol) (PS-*b*-PEG) coil–coil BCPs with high-molecular-weight polystyrene (PS) HPs, in which the molecular weight of the HPs is significantly larger than that of the PS blocks. The ratio of molecular weight of HPs to PS blocks, $r_{h/b}$, is up to more than 60 times. The preparation procedure is described as follows. The PS-*b*-PEG BCPs and the PS HPs were respectively dissolved in tetrahydrofuran/*N*,*N*′-dimethylformamide (THF/DMF) mixture solvent (3/7 by volume), and then the two solutions were mixed together to get stock solutions. The weight fraction of the HPs in the stock polymer mixtures (f_{HP}) varies from 0.1 to 0.95. By adding water to the solutions and subsequent dialysis against water, aggregate solutions in water were obtained. The influences of f_{HP} and $r_{h/b}$ on self-assembly morphology of various BCP/HP mixtures were investigated.

S. Zhang, Prof. C. Cai, Z. Xu, Prof. J. Lin, X. Jin
Shanghai Key Laboratory of Advanced Polymeric Materials
School of Materials Science and Engineering
East China University of Science and Technology
Shanghai 200237, China
E-mail: caichunhua@ecust.edu.cn; jlin@ecust.edu.cn

The ORCID identification number(s) for the author(s) of this article can be found under https://doi.org/10.1002/macp.201800443.

DOI: 10.1002/macp.201800443

2. Experimental Section

2.1. Materials and Regents

Styrene (St, Sigma-Aldrich, ≥99%) was washed with 5% NaOH aqueous solution and water successively, dried over anhydrous $CaCl_2$, and distilled twice from CaH_2 under reduced pressure to remove the inhibitor. Copper(I) bromide (CuBr, Sigma-Aldrich, 98%) was purified by stirring overnight with acetic acid at room temperature, filtrated, followed by washing with ethanol, diethyl ether, and acetone prior to drying under vacuum for 1 day. α-Methoxy-ω-hydroxy poly(ethylene glycol) (mPEG-OH, M_n = 5000), 2-bromo-2-methylpropionyl bromide (98%), ethyl 2-bromoisobutyrate (EBiB, 99%) and *N,N,N′,N′,N′*-pentamethyldiethylene triamine (PMDETA, 99%). THF, DMF, and all the other regents were used as received (purchased from Adamas-beta). Ultrahigh-molecular-weighted PS homopolymers (PS_{172k} and PS_{635k}) were purchased from Sigma-Aldrich. Deionized water was prepared in a Millipore Super-Q Plus Water System to a level of 18.2 MΩ cm resistance. Dialysis bag (Membra-cel, 3500 molecular weight cutoff) was provided by Serva Electrophoresis GmbH.

2.2. Synthesis of PS-*b*-PEG Block Copolymers and PS Homopolymers

PS-*b*-PEG BCPs and PS_{52k} (HPs) were synthesized by atom transition free radical polymerization (ATRP).[33,34] The typical procedure of ATRP of PS-*b*-PEG BCPs is as follows. First, the initiator (mPEG-Br, synthesized by the esterification of mPEG-OH and 2-bromo-2-methylpropionyl bromide according to the literature[35]) and styrene were added to a 50 mL Schlenk flask followed by addition of solvent (anisole). Next, PMDETA and CuBr were introduced and stirred together for 30 min. The solution was degassed by three cycles of freeze–pump–thaw to remove any dissolved oxygen and purged with dry nitrogen. The mixtures were stirred at 90 °C. After 5 h, the reaction mixtures were dissolved in THF and then passed through an Al_2O_3 column to remove the copper catalyst. The resulting solution was concentrated by rotary evaporation, and then was poured into a large volume of anhydrous methanol. The precipitated product was dried under vacuum and then purified twice by repeated precipitation from a THF solution into a large volume of anhydrous methanol. Finally, the product was dried under vacuum and white powder was collected. The synthesis of PS_{52k} HPs was similar to PS-*b*-PEG BCPs (EBiB as initiator and toluene as solvent).

The PS-*b*-PEG BCPs and PS_{52k} HPs were characterized by ^{1}H NMR (Avance 550, Bruker, $CDCl_3$ as solvent) and GPC (Waters 1515, THF as eluent solvent, PS as standard). For PS-*b*-PEG BCPs, since the degree of polymerization (DP) of the PEG block was known (112), the molecular weight of PS blocks can be calculated by peak intensities of phenyl group proton signal (6.8–7.1 ppm) of PS and the methylene proton signal (3.6 ppm) of PEG in the ^{1}H NMR spectrum. The molecular weight and polydispersity index (M_w/M_n) of both PS-*b*-PEG BCPs and PS HPs were determined by GPC. The characteristics of the polymers are listed in **Table 1**.

Table 1. Characteristics of polymers.

Polymer	M_n [kg mol^{-1}]	DP_{PS}	M_w/M_n[b)]
PS_{15k}-*b*-PEG_{5k}	20.1[a)]	145[a)]	1.11
PS_{10k}-*b*-PEG_{5k}	14.7[a)]	93[a)]	1.13
PS_{52k}	51.8[b)]	498[b)]	1.26
PS_{172k}	172.3[c)]	1657[c)]	1.24
PS_{635k}	635.2[c)]	6106[c)]	1.27

[a)]The M_n value and the degree of polymerization (DP) are derived according to GPC spectra in THF with PS as standard. The M_w/M_n values of the polymers are obtained from GPC testing; [b)]The M_n value and the degree of polymerization (DP) of PEG segment are known. The M_n and DP of PS block are derived according to ^{1}H NMR spectrum in $CDCl_3$; [c)]The samples are purchased from Sigma-Aldrich.

2.3. Preparation of Aggregates Self-Assembled from Polymer Mixtures

To prepare self-assemblies, the polymers were first dissolved in THF/DMF mixture solvent (3/7 by volume) by stirring at room temperature for 2 days to obtain stock solutions. The solutions of PS-*b*-PEG BCPs and PS HPs were mixed together with various proportions and then placed in a shaking incubator (100 rpm) for a day to obtain homogeneous solutions with the initial total concentration (C_0) of 0.2 g L^{-1}. To prepare micelle solution, 2 mL of deionized water, a selective solvent for PEG, was added to 4 mL of polymer mixture solution at a rate of 0.03 mL s^{-1} with vigorous stirring. Subsequently, all the solution was dialyzed against deionized water for 3 days to ensure that all the organic solvents were removed. Before further analysis, the solutions were stabilized for at least 5 days.

2.4. Characterizations and Measurements

2.4.1. Scanning Electron Microscopy

The morphologies of aggregates were observed by Scanning Electron Microscopy (SEM) (S4800, HITACHI) operated at an accelerating voltage of 15 kV. The samples were prepared by placing drops of solution on a silicon wafer surface and then dried at room temperature. Before the observations, the samples were sputtered by platinum.

2.4.2. Transmission Electron Microscopy

The morphologies of aggregates were also examined by Transmission Electron Microscopy (TEM) (JEM-1400, JEOL) operated at an accelerating voltage of 100 kV. Drops of solution were placed on a copper grid coated with carbon film and then dried at room temperature.

2.4.3. Atom Force Microscopy

The morphologies of aggregates were further examined by Atom Force Microscopy (AFM) measurements (XE-100, Park Systems) by using the non-contact mode at room temperature in air. The samples were prepared by placing drops of solution on a silicon wafer surface and then dried at room temperature.

2.4.4. Dynamic Light Scattering Measurements

Dynamic light scattering (DLS) was measured by an LLS spectrometer (ALV/CGS-5022F) equipped with an ALV-High QE APD detector and an ALV-5000 digital correlator using a He–Ne laser (the wavelength $\lambda = 632.8$ nm) as the light source. All the samples were filtered through 0.8 μm filters to remove dust before DLS measurements, and all the measurements were carried out at 25 °C and the scattering angle is 90°. From DLS testing, hydrodynamic radius (R_h) could be obtained.

2.4.5. Turbidity Measurements

Turbidity measurements (ODs) were performed to determine the critical water content (CWC) for the aggregate formation. Deionized water was then added drop by drop (0.02 mL per drop to 2 mL of polymer solution) with vigorous stirring. And after each drop of deionized water was added, the solution was stirred for 1 min and then left to equilibrate for 2 min or more until the optical density was stable. The turbidity (UV absorbance) was measured at a wavelength of 690 nm (which was far from the absorption of the benzene chromophore) using a quartz cell (path length: 1 cm) with a UV–vis spectrophotometer (UV–vis UV-2550 SHIMADZU).

3. Results and Discussion

We first studied the self-assembly behavior of PS_{15k}-*b*-PEG_{5k}/PS_{52k} (subscripts denote the molecular weight of each segment) mixtures ($r_{h/b} \approx 3.5$). As shown in **Figure 1**a, both SEM and TEM (inset) images reveal that PS_{15k}-*b*-PEG_{5k} BCPs form spherical micelles with uniform diameter about 34 nm. When a small amount of PS_{52k} HPs was incorporated (Figure 1b, $f_{HP} = 0.10$), spherical aggregates with diameter about 50 nm appeared. The inset TEM image indicates a solid structure of these swollen spheres. Increasing f_{HP} to 0.20, vesicles with diameter about 120 nm were observed (Figure 1c). As shown in the inset TEM image, the thickness of the vesicular wall is non-uniform, which is different from the typical vesicles formed by pure BCPs.[36] In addition, different contrasts in the vesicular wall were observed suggesting phase separation of PS chains of BCPs and HPs.[37] AFM testing was also applied to characterize these vesicles (Figure 1d). According to the AFM image, the diameter of the vesicles is about 180 nm and the height is about 12 nm. Such difference between the diameter and the height is due to the soft characteristic of the vesicular wall.[38,39] As more PS_{52k} HPs were added, rod-like aggregates can be observed (Figure 1e, $f_{HP} = 0.40$). The width of the rods is about 50 nm, and their length varies from 100 to 300 nm. Further increasing f_{HP} leads to large spherical aggregates. The diameter of these large spheres increases with f_{HP} from about 150 nm (Figure 1f, $f_{HP} = 0.60$) to about 300 nm (Figure 1g, $f_{HP} = 0.95$). In addition to the morphology transitions, it should be note that small spherical micelles formed by PS_{15k}-*b*-PEG_{5k} BCPs are always observed in these systems, and the portion of these micelles decreases with increasing f_{HP}. For the system prepared with ultrahigh f_{HP} (Figure 1g, $f_{HP} = 0.95$), small spherical micelles are hardly observed.

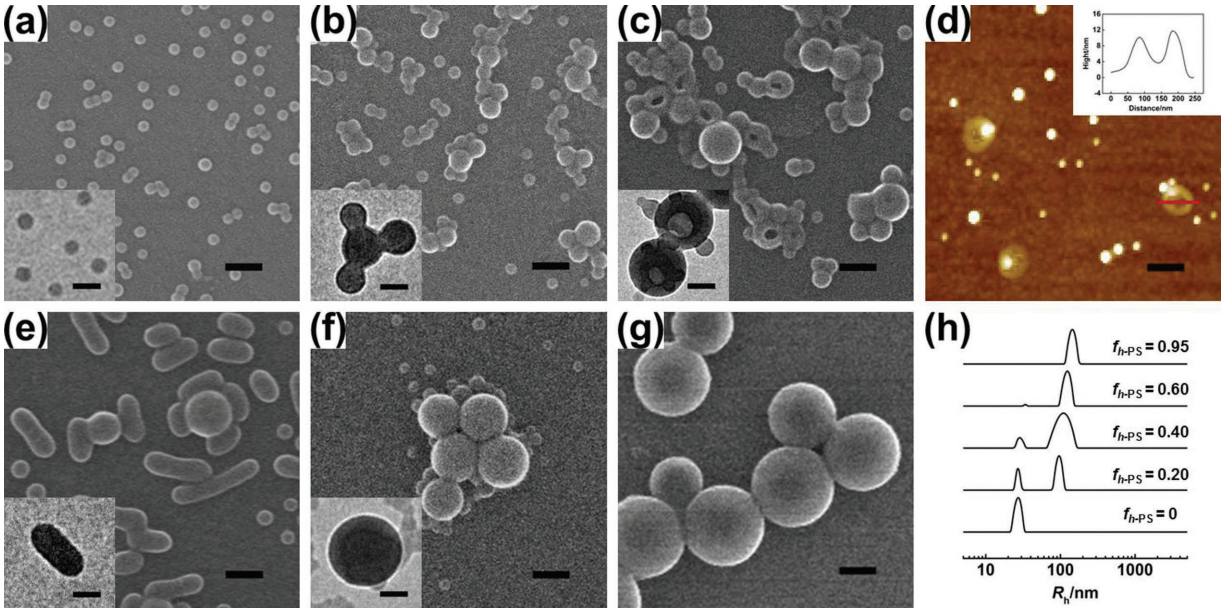

Figure 1. SEM images of aggregates formed by PS_{15k}-*b*-PEG_{5k}/PS_{52k} mixtures ($r_{h/b} \approx 3.5$) with various f_{HP}: a) 0, b) 0.10, c) 0.20, e) 0.40, f) 0.60, and g) 0.95 (insets are TEM images for the corresponding samples). d) AFM image of aggregates formed by PS_{15k}-*b*-PEG_{5k}/PS_{52k} mixtures with $f_{HP} = 0.20$ (inset shows the height profile along the red line). h) Typical R_h distributions of aggregates self-assembled from PS_{15k}-*b*-PEG_{5k}/PS_{52k} mixtures with various f_{HP}. Scale bars: 100 nm in (a–c and e–g), 200 nm in (d), and insets: 50 nm.

Such morphology transitions as a function of f_{HP} were further monitored by DLS measurement. The typical hydrodynamic radius (R_h) distributions are displayed in Figure 1h. It was found that PS_{15k}-*b*-PEG_{5k} micelles have a mean R_h value about 24 nm and possess a narrow size distribution. The DLS result for the size of the micelles is slightly larger than that of SEM and TEM observations. The reason is that DLS testing reflects the "real" state of the micelles in solution, while SEM and TEM show the micelles in dry state.[40] For the aggregates formed by PS_{15k}-*b*-PEG_{5k}/PS_{52k} mixtures, a new peak in the right position (with higher R_h value) appeared which corresponds to the hybrid aggregates. As shown in Figure 1h, with increasing f_{HP} from 0.20 to 0.60, the mean R_h value of the right peak shifts from 89 to 123 nm, corresponding to the vesicle–rod–large sphere morphology transition. The relative area of the left peak significantly decreases, indicating fewer PS_{15k}-*b*-PEG_{5k} micelles existed in the solution. For mixtures with f_{HP} = 0.95, only one peak with R_h value about 160 nm was observed. These DLS results clearly demonstrate the self-assembly features of the PS_{15k}-*b*-PEG_{5k}/PS_{52k} mixtures as observed by SEM and TEM observations.

We then investigated the self-assembly behavior of PS_{15k}-*b*-PEG_{5k}/PS mixtures with higher $r_{h/b}$ values by increasing the molecular weight of PS HPs. It was found that for the system with $r_{h/b} \approx 11$ (PS_{15k}-*b*-PEG_{5k}/PS_{172k} mixtures), similar to that of the system with $r_{h/b} \approx 3.5$ (PS_{15k}-*b*-PEG_{5k}/PS_{52k} mixtures), vesicles, rod-like aggregates, and large spheres are observed successively with increasing f_{HP} (Figure S1, Supporting Information). For the system with $r_{h/b} \approx 42$ (PS_{15k}-*b*-PEG_{5k}/PS_{635k} mixtures), vesicles are formed at f_{HP} = 0.20 (**Figure 2**a). While large spherical aggregates could be formed at a relative lower f_{HP} (f_{HP} = 0.40–0.95, Figure 2b–d). In addition, PS_{10k}-*b*-PEG_{5k} was applied to cooperatively self-assemble with these PS HPs ($r_{h/b} \approx$ 5–63). It was found that stable aggregates including vesicles and large spheres can still be prepared. The morphology transitions of PS_{10k}-*b*-PEG_{5k}/PS_{635k} mixtures were taken as an example to illustrate such self-assembly behaviors (Figure S2, Supporting Information).

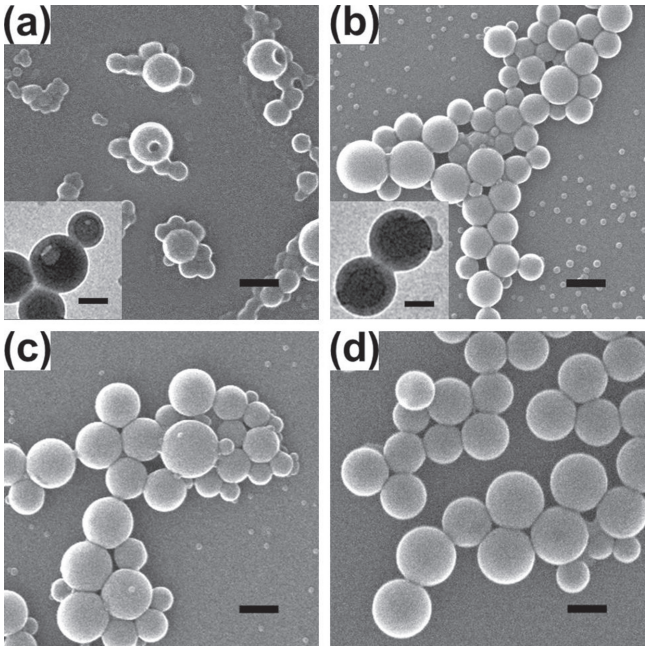

Figure 2. SEM images of aggregates formed by PS_{15k}-*b*-PEG_{5k}/PS_{635k} mixtures ($r_{h/b} \approx 42$) with various f_{HP}: a) 0.20, b) 0.40, c) 0.60, and d) 0.95 (insets are TEM images for the corresponding samples). Scale bars: 200 nm, and insets: 100 nm.

Next, we examined the dispersing stability of the aggregates by monitoring the turbidity (optical density) of the solutions (Figure S3, Supporting Information). It was found that the solutions of relatively smaller aggregates show high stability. No apparent decrease of the absorbance value was observed after being stored for 6 months. For solutions of relatively larger aggregates, the absorbance value decreases slightly with increasing storing time, indicating the settlement of part of large aggregates. Note that these settled aggregates can be re-dispersed in the aqueous solution by gentle shaking. Such phenomena could be assigned to the lower weight fraction of hydrophilic PEG block in these larger aggregates. In addition, all the aggregates show high stability in structures, they retain their morphologies after being stored for more than 6 months (Figure S4, Supporting Information).

To gain deep insight into the cooperatively self-assembly behaviors, the dynamic aggregation processes of the BCPs, homopolymers, and polymer mixtures against added water content were investigated. First, the turbidity of solutions of PS_{15k}-*b*-PEG_{5k} (0.16 g L^{-1}), PS_{52k} (0.04 g L^{-1}), and PS_{15k}-*b*-PEG_{5k}/PS_{52k} mixtures (0.2 g L^{-1}, f_{HP} = 0.20) versus added water content was monitored. According to the turbidity curves, CWC values indicated by the sudden increase of turbidity can be obtained.[41] The CWC value of the PS-*b*-PEG BCPs corresponds to the onset of the self-assembly, while the CWC value of the PS HPs reflects the onset of the collapse of the chains into globules.[42,43] As shown in **Figure 3**a, the CWC values for the PS_{15k}-*b*-PEG_{5k} and PS_{52k} are 18.5 and 5.2 vol%, respectively. For the solution of PS_{15k}-*b*-PEG_{5k}/PS_{52k} mixtures, the CWC value (5.7 vol%) is slightly larger than that of the PS_{52k} solution, and the turbidity remains nearly constant with further increasing water content. According to these results, it is reasonable to believe that PS_{52k} HPs would first collapse into globules which further self-assemble with PS_{15k}-*b*-PEG_{5k} BCPs due to the distinction of CWC values of PS_{52k} solution and PS_{15k}-*b*-PEG_{5k} solution. Additionally, in the solution of PS_{15k}-*b*-PEG_{5k}/PS_{52k} mixtures, the BCPs not only delayed the collapse of HP chains into globules, but also stabilized these globules from precipitating due to the attractions between the BCPs and HPs such as hydrophobic–hydrophobic and π–π interactions.[30–32]

The stabilization of the PS_{52k} globules by PS_{15k}-*b*-PEG_{5k} is evidenced by DLS testing (Figure 3b). As can be seen, for both solutions of PS_{52k} (0.04 g L^{-1}) and PS_{15k}-*b*-PEG_{5k}/PS_{52k} mixtures (0.2 g L^{-1}, f_{HP} = 0.20), when the water content is lower than 5.0 vol%, the R_h values are about 8 nm, which correspond to the free polymer chains in solution. For the PS_{52k} solution (0.04 g L^{-1}), the R_h value increases to tens of nanometers with the water content surpassing 5.4 vol%, which indicates that PS_{52k} homopolymers aggregate into globules. Further adding water would induce remarkable increase in R_h value due to rapid aggregation of the initially formed PS_{52k} globules. While for the PS_{15k}-*b*-PEG_{5k}/PS_{52k} mixture solution (0.2 g L^{-1}, f_{HP} = 0.20), the R_h value

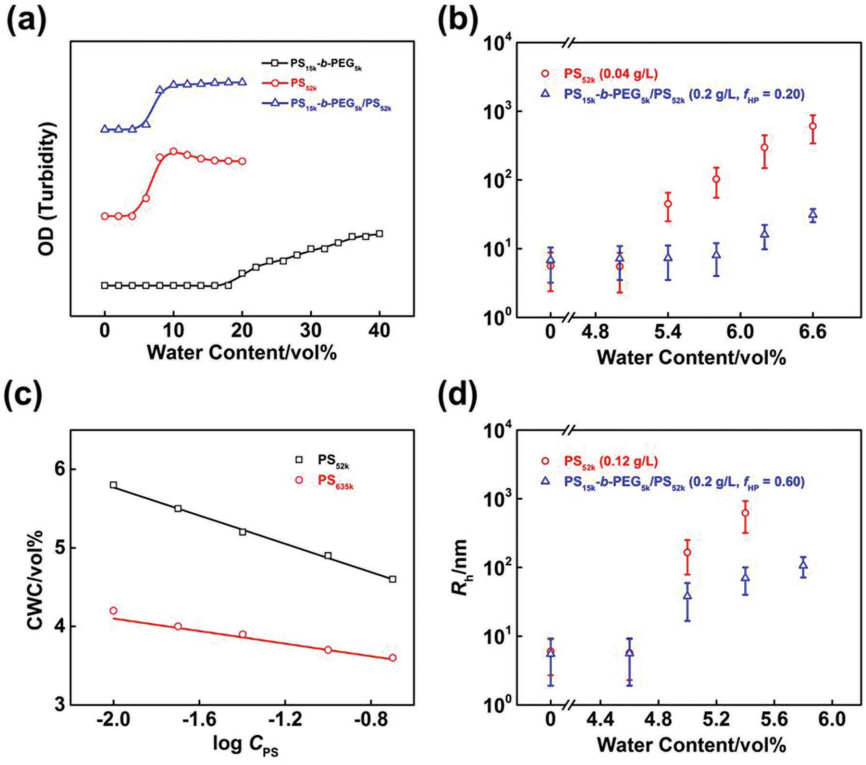

Figure 3. a) Turbidity (optical density) curves of solutions of PS_{15k}-*b*-PEG_{5k} (0.16 g L^{-1}), PS_{52k} (0.04 g L^{-1}), and PS_{15k}-*b*-PEG_{5k}/PS_{52k} mixtures (0.2 g L^{-1}, f_{HP} = 0.20) as a function of the added water content. b) Plots of R_h values versus the added water content for PS_{52k} (0.04 g L^{-1}) and PS_{15k}-*b*-PEG_{5k}/PS_{52k} mixtures (0.2 g L^{-1}, f_{HP} = 0.20). c) Plots of CWC values versus the logarithm of the concentration of PS_{52k} and PS_{635k}. d) Plots of R_h versus the added water content for PS_{52k} (0.12 g L^{-1}) and PS_{15k}-*b*-PEG_{5k}/PS_{52k} mixtures (0.2 g L^{-1}, f_{HP} = 0.60). Scattering angle is 90°.

is much smaller than that of the PS_{52k} solution (0.04 g L^{-1}) at the same added water content. These results clearly indicated that the PS_{15k}-*b*-PEG_{5k} can stabilize the PS_{52k} globules and prevent further rapid aggregation. Accordingly, the self-assembly process can be regarded as a cooperative self-assembly of the BCPs with the pre-formed PS globules.

In addition, as shown in Figure 3c, the CWC value of the PS_{52k} solutions decreases with increasing concentration, and PS_{635k} with higher molecular weight possesses lower CWC value at corresponding polymer concentration. The lower the CWC value, the larger the globule formed at corresponding added water content. For example, in the case of PS_{15k}-*b*-PEG_{5k}/PS_{52k} mixture solution (0.2 g L^{-1}) with water content of 5.8 vol%, the size of the PS globules in the system with f_{HP} = 0.6 is about ten times larger than that in the system with f_{HP} = 0.2 (Figure 3b vs Figure 3d). Since the morphology of the aggregates varies greatly with the f_{HP} (Figure 1) and the molecular weight of the homopolymer (Figure 1e vs Figure 2b), the size of the PS globules should be a key factor influencing the self-assembly behaviors.

Based on these experimental findings, possible mechanisms regarding the cooperative self-assembly of PS-*b*-PEG (typically, PS_{15k}-*b*-PEG_{5k}) BCPs and high-molecular-weight PS HPs are proposed. As illustrated in **Scheme 1**, the self-assembly process can be divided into two successive steps. With adding water to the initial solution of the polymer mixtures, PS_{52k} HPs first collapse and form globules which are stabilized by PS_{15k}-*b*-PEG_{5k} BCPs.[44] Subsequently, with further adding water, the pre-formed PS globules would cooperative self-assemble with PS_{15k}-*b*-PEG_{5k} BCPs. Moreover, the morphology of aggregates is determined by the size of PS globules, which is related to f_{HP}. When f_{HP} is lower, the size of the pre-formed PS globules is small (in the scale of 10 nm). In the further cooperative self-assembly, the small globules could increase the volume fraction of hydrophobic blocks, leading to the formation a morphology transition from spherical to vesicle with a less curved interface (Scheme 1a).[44,45] With increasing f_{HP}, rod-like aggregates can be produced (Scheme 1b). For the formation of such interesting morphology, the probable reason is explained as follows. With increase of f_{HP}, both the number and size of these pre-formed PS globules increase.[46] In such a situation, the adjacent PS globules are easier to fuse with each

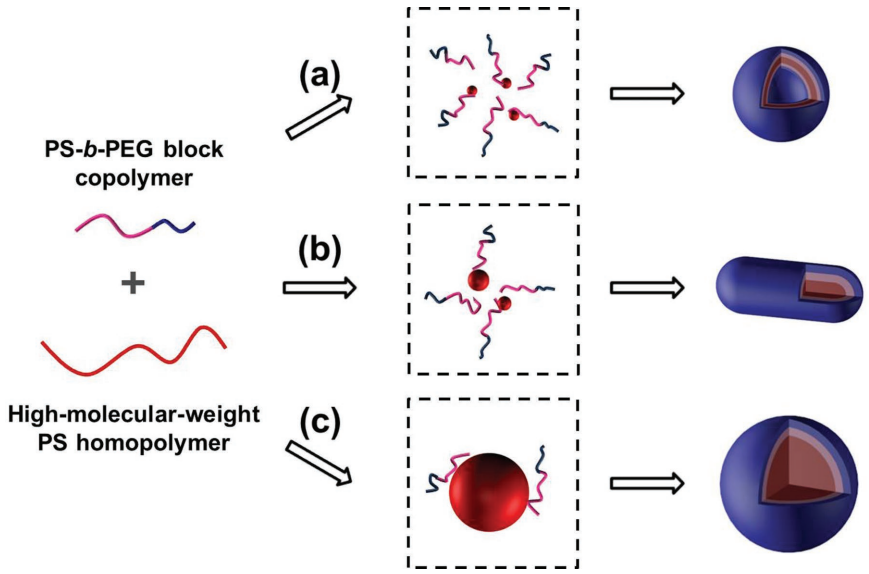

Scheme 1. A schematic illustration for the two-step self-assembly of PS-*b*-PEG/PS mixtures. a) Vesicles formed at relatively lower f_{HP}; b) Rod-like aggregates formed with increasing f_{HP}; c) Large spheres formed at relatively higher f_{HP}.

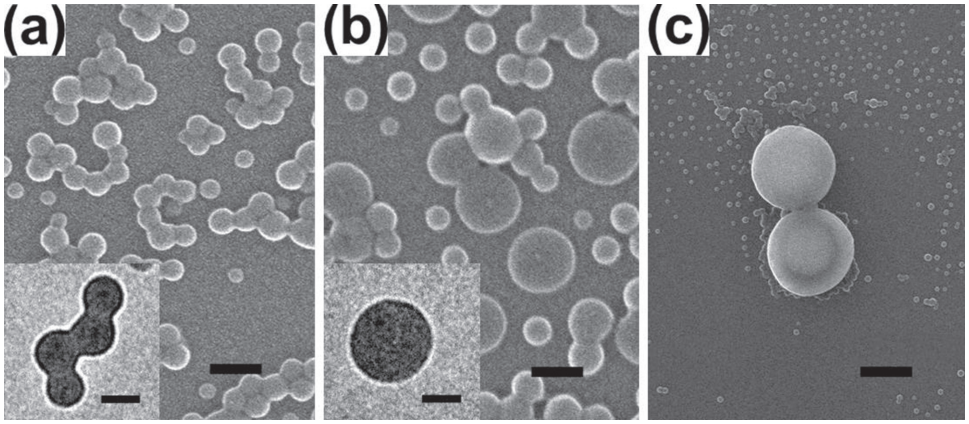

Figure 4. SEM images of aggregates formed by PS_{15k}-*b*-PEG_{5k}/AuNPs mixtures with various f_{AuNPs}: a) 0.20, and b) 0.40 (insets are TEM images for the corresponding samples). c) SEM images of aggregates formed by PS_{15k}-*b*-PEG_{5k}/PSMPs mixtures with f_{PSMPs} = 0.60. Scale bars: 200 nm in (a,b), 400 nm in (c), and insets: 100 nm.

other forming rod-like aggregates upon water addition. In fact, fusion of polymer particles into new morphologies has already been reported in several works.[44,47,48] Further increasing f_{HP} produces large globules (in the scale of 100 nm) which act as templates for the PS_{15k}-*b*-PEG_{5k} BCPs. As a result, large spheres were yielded (Scheme 1c).[49,50] In addition to the f_{HP}, the size of the PS globules also increases with their molecular weight. Therefore, in the case of PS-*b*-PEG/PS_{635k} mixtures, large spheres are obtained with lower f_{HP} than that of the PS-*b*-PEG/PS_{52k} mixtures.

To further specify the mechanisms of cooperative self-assembly of PS_{15k}-*b*-PEG_{5k} with PS homopolymer globules, control experiments that cooperative self-assembly of PS_{15k}-*b*-PEG_{5k} with small gold nanoparticles (AuNPs, diameter about 6 nm) or large PS microparticles (PSMPs, diameter about 500 nm) were conducted (for the synthesis of the AuNPs and PSMPs, see Supporting Information). For the PS_{15k}-*b*-PEG_{5k}/AuNPs mixtures, swollen spheres and vesicles are formed with f_{AuNPs} = 0.20 (**Figure 4**a) and f_{AuNPs} = 0.40 (Figure 4b), respectively. These AuNPs act as modifiers similar to the small PS globules as observed in the PS_{15k}-*b*-PEG_{5k}/PS mixtures with low f_{HP}. For the mixtures of PS_{15k}-*b*-PEG_{5k} and PSMPs, large spheres are always observed, in which the PSMPs serve as templates mimicking the larger PS globules in the self-assembly of PS_{15k}-*b*-PEG_{5k}/PS mixtures with high f_{HP}. Figure 4c shows typical morphology of aggregates formed with f_{PSMPs} = 0.60. These results support the proposed mechanisms for the self-assembly behaviors of the PS-*b*-PEG/PS mixtures well, and enhance the understanding on such self-assembly behaviors.

The present work reports for the first time that coil–coil BCPs can cooperatively self-assemble with high-molecular-weight flexible HPs into stable aggregates. This study expands the research scope and promotes better understanding of the self-assembly behavior of polymer mixtures. The gained information could provide useful guidance in regulating the morphology of BCPs aggregates. Furthermore, this work provides a facile way, that is cooperative self-assembly with BCPs, to remarkably enhance the solubility of high-molecular-weight HPs in bad solvents, which could facilitate the applications of these high-molecular-weight HPs.

4. Conclusions

In summary, the cooperative self-assembly of PS-*b*-PEG BCPs with PS HPs has been studied, in which the molecular weight of PS HPs is much larger than that of the PS blocks. With increasing weight fraction of PS HPs in the polymer mixtures, vesicles and large spheres are successively formed. The PS HPs in the cooperative self-assembly process are in the form of globules with their size depending on f_{HP}. For mixtures with low f_{HP}, the PS HPs formed small globules which cooperatively self-assemble with the PS-*b*-PEG BCPs into vesicles. For mixtures with high f_{HP}, the PS HPs formed large globules acting as self-assembly templates for the BCPs, and large spheres are produced.

Supporting Information

Supporting Information is available from the Wiley Online Library or from the author.

Acknowledgements

This work was supported by the National Natural Science Foundation of China (51573049 and 21474029).

Conflict of Interest

The authors declare no conflict of interest.

Keywords

block copolymers, homopolymers, morphology modifiers, self-assembly, templates

Received: October 8, 2018
Revised: November 26, 2018
Published online: December 13, 2018

[1] L. Wang, X. Yu, S. Yang, J. X. Zheng, R. M. Van Horn, W.-B. Zhang, J. Xu, S. Z. D. Cheng, *Macromolecules* **2012**, *45*, 3634.
[2] Z. Lin, S. Liu, W. Mao, H. Tian, N. Wang, N. Zhang, F. Tian, L. Han, X. Feng, Y. Mai, *Angew. Chem. Int. Ed.* **2017**, *56*, 7135.
[3] Z. Lin, H. Tian, F. Xu, X. Yang, Y. Mai, X. Feng, *Polym. Chem.* **2016**, *7*, 2092.
[4] W. Tao, Y. Liu, B. Jiang, S. Yu, W. Huang, Y. Zhou, D. Yan, *J. Am. Chem. Soc.* **2012**, *134*, 762.
[5] E. Baba, T. Yatsunami, Y. Tezuka, T. Yamamoto, *Langmuir* **2016**, *32*, 10344.
[6] R. Deng, F. Liang, X. Qu, Q. Wang, J. Zhu, Z. Yang, *Macromolecules* **2015**, *48*, 750.
[7] M. Zhu, H. Kim, Y. J. Jang, S. Park, D. Y. Ryu, K. Kim, P. Tang, F. Qiu, D. H. Kim, J. Peng, *J. Mater. Chem. A* **2016**, *4*, 18432.
[8] X. Hu, J. Hu, J. Tian, Z. Ge, G. Zhang, K. Luo, S. Liu, *J. Am. Chem. Soc.* **2013**, *135*, 17617.
[9] L. Su, C. Wang, F. Polzer, Y. Lu, G. Chen, M. Jiang, *ACS Macro Lett.* **2014**, *3*, 534.
[10] J. Xue, Z. Guan, J. Lin, C. Cai, W. Zhang, X. Jiang, *Small* **2017**, *13*, 1604214.
[11] C. Cai, J. Lin, Y. Lu, Q. Zhang, L. Wang, *Chem. Soc. Rev.* **2016**, *45*, 5985.
[12] J. Tan, D. Chong, Y. Zhou, R. Wang, X. Wan, J. Zhang, *Langmuir* **2018**, *34*, 8975.
[13] J. Yang, Y. Hu, R. Wang, D. Xie, *Soft Matter* **2017**, *13*, 7840.
[14] F. Xu, D. Wu, Y. Huang, H. Wei, Y. Gao, X. Feng, D. Yan, Y. Mai, *ACS Macro Lett.* **2017**, *6*, 426.
[15] W. Li, X. Zhu, J. Wang, R. Liang, J. Li, S. Liu, G. Tu, J. Zhu, *J. Colloid Interface Sci.* **2014**, *418*, 81.
[16] W. Agut, A. Brûlet, C. Schatz, D. Taton, S. Lecommandoux, *Langmuir* **2010**, *26*, 10546.
[17] Y. Han, C. Cai, J. Lin, S. Gong, W. Xu, R. Hu, *Macromol. Rapid Commun.* **2018**, *39*, 1800080.
[18] Y. Mai, A. Eisenberg, *Chem. Soc. Rev.* **2012**, *41*, 5969.
[19] G. Cambridge, M. J. Gonzalez-Alvarez, G. Guerin, I. Manners, M. A. Winnik, *Macromolecules* **2015**, *48*, 707.
[20] T. Mori, T. Watanabe, K. Minagawa, M. Tanaka, *J. Polym. Sci., Part A: Polym. Chem.* **2005**, *43*, 1569.
[21] G. Rizis, T. G. M. van de Ven, A. Eisenberg, *ACS Nano* **2015**, *9*, 3627.
[22] Y. Hirai, T. Wakiya, H. Yabu, *Polym. Chem.* **2017**, *8*, 1754.
[23] S. Lin, Y. Wang, C. Cai, Y. Xing, J. Lin, T. Chen, X. He, *Nanotechnology* **2013**, *24*, 085602.
[24] L. Lei, J.-F. Gohy, N. Willet, J.-X. Zhang, S. Varshney, R. Jérôme, *Polymer* **2004**, *45*, 4375.
[25] N. Ouarti, P. Viville, R. Lazzaroni, E. Minatti, M. Schappacher, A. Deffieux, R. Borsali, *Langmuir* **2005**, *21*, 1180.
[26] G.-K. Xu, X.-Q. Feng, Y. Li, *J. Phys. Chem. B* **2010**, *114*, 1257.
[27] A. Dehghan, A.-C. Shi, *Macromolecules* **2013**, *46*, 5796.
[28] J. F. Reuther, D. A. Siriwardane, R. Campos, B. M. Novak, *Macromolecules* **2015**, *48*, 6890.
[29] O. V. Kulikov, D. A. Siriwardane, J. F. Reuther, G. T. McCandless, H. Sun, Y. Li, S. F. Mahmood, S. S. Sheiko, V. Percec, B. M. Novak, *Macromolecules* **2015**, *48*, 4088.
[30] C. Cai, Y. Li, J. Lin, L. Wang, S. Lin, X.-S. Wang, T. Jiang, *Angew. Chem. Int. Ed.* **2013**, *52*, 7732.
[31] C. Cai, J. Lin, X. Zhu, S. Gong, X.-S. Wang, L. Wang, *Macromolecules* **2016**, *49*, 15.
[32] S. Zhang, C. Cai, Q. Huang, J. Lin, Z. Xu, *Acta Polym. Sin.* **2018**, 109.
[33] K. Matyjaszewski, J. Xia, *Chem. Rev.* **2001**, *101*, 2921.
[34] X. He, L. Liang, M. Xie, Y. Zhang, S. Lin, D. Yan, *Macromol. Chem. Phys.* **2007**, *208*, 1797.
[35] W. Yuan, J. Zhang, J. Wei, C. Zhang, J. Ren, *Eur. Polym. J.* **2011**, *47*, 949.
[36] J. Du, Y. Chen, Y. Zhang, C. C. Han, K. Fischer, M. Schmidt, *J. Am. Chem. Soc.* **2003**, *125*, 14710.
[37] S. Wu, L. Wang, A. Kroeger, Y. Wu, Q. Zhang, C. Bubeck, *Soft Matter* **2011**, *7*, 11535.
[38] M. Yang, W. Wang, F. Yuan, X. Zhang, J. Li, F. Liang, B. He, B. Minch, G. Wegner, *J. Am. Chem. Soc.* **2005**, *127*, 15107.
[39] J. Sun, X. Chen, C. Deng, H. Yu, Z. Xie, X. Jing, *Langmuir* **2007**, *23*, 8308.
[40] C. Stoffelen, J. Voskuhl, P. Jonkheijm, J. Huskens, *Angew. Chem. Int. Ed.* **2014**, *53*, 3400.
[41] S. Zhang, C. Cai, Z. Guan, J. Lin, X. Zhu, *Chin. Chem. Lett.* **2017**, *28*, 839.
[42] T. I. Morozova, A. Nikoubashman, *J. Phys. Chem. B* **2018**, *122*, 2130.
[43] J. M. Polson, N. E. Moore, *J. Chem. Phys.* **2005**, *122*, 024905.
[44] D. Li, X. Jia, X. Cao, T. Xu, H. Li, H. Qian, L. Wu, *Macromolecules* **2015**, *48*, 4104.
[45] R. J. Hickey, A. S. Haynes, J. M. Kikkawa, S.-J. Park, *J. Am. Chem. Soc.* **2011**, *133*, 1517.
[46] L. Zhang, A. Eisenberg, *Macromolecules* **1999**, *32*, 2239.
[47] Z. Zhuang, T. Jiang, J. Lin, L. Gao, C. Yang, L. Wang, C. Cai. *Angew. Chem. Int. Ed.* **2016**, *55*, 12522.
[48] C. Yang, X. Ma, J. Lin, L. Wang, Y. Lu, L. Zhang, C. Cai, L. Gao, *Macromol. Rapid Commun.* **2018**, *39*, 1700701.
[49] W. Hou, Y. Feng, B. Li, H. Zhao, *Macromolecules* **2018**, *51*, 1894.
[50] J. Rao, H. Zhang, S. Gaan, S. Salentinig, *Macromolecules* **2016**, *49*, 5978.